Received: 9 October 2017 | Accepted: 23 October 2017

DOI: 10.1002/prp2.374

ORIGINAL ARTICLE

Distortion of K_B estimates of endothelin-1 ET_A and ET_B receptor antagonists in pulmonary arteries: Possible role of an endothelin-1 clearance mechanism

James A. Angus[1] | Richard J. A. Hughes[1] | Christine E. Wright[1]

Cardiovascular Therapeutics Unit, Department of Pharmacology and Therapeutics, University of Melbourne, Melbourne, Vic., Australia

Correspondence
James A. Angus, Cardiovascular Therapeutics Unit, Department of Pharmacology and Therapeutics, University of Melbourne, Vic., Australia.
Email: jamesaa@unimelb.edu.au

Abstract

Dual endothelin ET_A and ET_B receptor antagonists are approved therapy for pulmonary artery hypertension (PAH). We hypothesized that ET_B receptor-mediated clearance of endothelin-1 at specific vascular sites may compromise this targeted therapy. Concentration-response curves (CRC) to endothelin-1 or the ET_B agonist sarafotoxin S6c were constructed, with endothelin receptor antagonists, in various rat and mouse isolated arteries using wire myography or in rat isolated trachea. In rat small mesenteric arteries, bosentan displaced endothelin-1 CRC competitively indicative of ET_A receptor antagonism. In rat small pulmonary arteries, bosentan 10 μmol L^{-1} left-shifted the endothelin-1 CRC, demonstrating potentiation consistent with antagonism of an ET_B receptor-mediated endothelin-1 clearance mechanism. Removal of endothelium or L-NAME did not alter the EC_{50} or Emax of endothelin-1 nor increase the antagonism by BQ788. In the presence of BQ788 and L-NAME, bosentan displayed ET_A receptor antagonism. In rat trachea (ET_B), bosentan was a competitive ET_B antagonist against endothelin-1 or sarafotoxin S6c. Modeling showed the importance of dual receptor antagonism where the potency ratio of ET_A to ET_B antagonism is close to unity. In conclusion, the rat pulmonary artery is an example of a special vascular bed where the resistance to antagonism of endothelin-1 constriction by ET dual antagonists, such as bosentan or the ET_B antagonist BQ788, is possibly due to the competition of potentiation of endothelin-1 by blockade of ET_B-mediated endothelin-1 clearance located on smooth muscle and antagonism of ET_A- and ET_B-mediated contraction. This conclusion may have direct application for the efficacy of endothelin-1 antagonists for treating PAH.

KEYWORDS

ambrisentan, bosentan, BQ788, endothelin-1, ET_A receptors, ET_B receptor-mediated clearance mechanism, ET_B receptors, macitentan, sarafotoxin S6c

Abbreviations: D_{100}, artery (mesenteric or tail) internal diameter (μm) at an equivalent transmural pressure of 100 mm Hg; D_{20}, artery (pulmonary) internal diameter (μm) at an equivalent transmural pressure of 20 mm Hg; Emax, maximum possible effect for the agonist; KPSS, isotonic potassium physiological salt solution (K^+ 124 mmol L^{-1} for arteries or K^+ 62 mmol L^{-1} for trachea); pEC_{50}, negative $\log_{10}$ M concentration of agonist that evokes the half-maximal response; pK_B, negative $\log_{10}$ M concentration of antagonist that shifted the agonist endothelin-1 EC_{50} twofold to the right; PSS, physiological salt solution.

1 | INTRODUCTION

In rats,[1] rabbits,[2] and nonhuman primates,[3] dual ET_A and ET_B receptor antagonists or ET_B-selective endothelin-1 antagonists increased the immunoreactive endothelin-1 plasma level acutely by 3- to 10-fold. After chronic oral dosing in rats with A-182086, a dual ET_A and ET_B antagonist, the endothelin-1 plasma levels rose by more than 24-fold after 9 days.[4] Micro positron emission tomography using ^{18}F-labeled endothelin-1 in anesthetized rats confirmed that endothelin-1 rapidly binds to rat lung and is cleared from the circulation ($t_{0.5}$ 0.43 minutes).[5] Pretreatment with the ET_B-selective antagonist BQ788 decreased the endothelin-1 clearance by 85%.

While this intriguing mechanism of endothelin-1 clearance by ET_B receptors was first determined in vivo, we asked, could this mechanism affect the pharmacodynamics of endothelin-1 interactions with ET_A and ET_B receptors mediating smooth muscle contraction in isolated tissue assays when determining the pK_B of endothelin-1 receptor antagonists? The impact of sites of loss of agonist or antagonist concentrations on pK_B estimations has been observed in the acid-secreting mouse stomach (figure 1 in Angus and Black[6]) and further developed by Kenakin.[7] Indeed, we have previously reported that endothelin-1 concentration-contraction curves in rat small interlobar pulmonary arteries were surprisingly LEFT-shifted; ie, endothelin-1 contractions were "potentiated" in the presence of the dual ET_A and ET_B antagonist bosentan 10 μmol L^{-1},[8] an observation that is consistent with blockade of a site of loss of endothelin-1.

Here, we report the pharmacodynamic interactions and analyses of endothelin-1 receptor antagonists in a range of isolated arteries and tracheal smooth muscle preparations with endothelin-1 and the selective ET_B receptor agonist venom peptide sarafotoxin S6c. Some arteries were treated with L-NAME or had the endothelial cell layer removed. Our results show that the localized ET_B clearance mechanism for endothelin-1 on smooth muscle cells could explain the dramatic effect on the estimation of the dissociation constant for ET_A and ET_B antagonists when endothelin-1 is used as the agonist and the endothelin-1 clearance mechanism is present.

The conclusions provide a theoretical framework to test for the "ideal" dual ET_A and ET_B receptor antagonist if significant antagonism is to occur at ET_A or ET_B constrictor receptors and the ET_B receptor-mediated clearance of endothelin-1 is blocked which potentiates the potency of endothelin-1. This clearance mechanism, thus, joins other well-known mechanisms of ET_B-mediated endothelin-1 release of thromboxane A_2, prostacyclin, and nitric oxide that would either enhance or functionally antagonize ET_A- or ET_B-mediated vasoconstriction.[9-12]

2 | MATERIALS AND METHODS

The ethics committee of the University of Melbourne approved the experiments in accordance with the *Australian Code for the Care and Use of Animals for Scientific Purposes* (8th edition, 2013; National Health & Medical Research Council, Canberra, Australia). Animal studies are reported in compliance with the ARRIVE guidelines.[13,14] Male Sprague-Dawley rats (280-320 g; Biomedical Sciences Animal Facility, University of Melbourne, Australia) and male Swiss mice (30-40 g; Animal Resources Centre, Murdoch, WA, Australia) were used in this study. Animals were housed (3-4 per high-topped cage with shredded paper bedding) at 22°C on a 12-hour light/dark cycle with access to food and water ad libitum. Rats and mice were individually placed in a secure chamber and deeply anesthetized by inhalation of 5% isoflurane in oxygen, then killed by rapid excision of the heart. The rat and mouse tissues were rapidly excised and placed in cold physiological salt solution (PSS) with the following composition (mM): NaCl 119; KCl 4.69; $MgSO_4.7H_2O$ 1.17; KH_2PO_4 1.18; glucose 5.5; $NaHCO_3$ 25; $CaCl_2.6H_2O$ 2.5; EDTA 0.026 and saturated with carbogen (O_2 95%; CO_2 5%) at pH 7.4. Tissues were pinned down on a Silastic-covered petri dish filled with cold PSS. A minimum of 5 rats or mice was used for each experimental group, with exact *n* values shown in the figure legends or Results section. Group sizes were equal by design; however, variations due to predetermined criteria (described in the methodology) are explained in the figure legends. Animal tissues were randomized to treatment groups.

2.1 | Arteries

As previously described,[15] third-order rat and mouse mesenteric arteries, rat and mouse pulmonary arteries, and mouse tail arteries were dissected clear of their connective tissue and prepared as 2-mm-long segments for mounting on 40-μm diameter wires for isometric force measurement in Mulvany and Halpern style myographs (model 620M, Danish Myo Technology, Aarhus, Denmark). Responses were captured by a Powerlab 4/30 A/D converter (ADInstruments, Sydney, Australia) and measured on a computer running LabChart 7 data acquisition software (ADInstruments).

After 30-minute equilibration in PSS at 37°C, the arteries were passively stretched under micrometer (Mitutoyo, Kawasaki, Japan) control according to the normalization protocol to determine the internal diameter at equivalent transmural pressure of 100 mm Hg (D_{100}) for all arteries, except for the pulmonary artery where 20 mm Hg was used (D_{20}). The micrometer was then adjusted to decrease the passive stretch to an equivalent diameter of 90% of D_{100} (or 90% of D_{20}, as applicable) and the artery remained at that setting of passive stretch for the remainder of the experiment.[15,16] Thirty minutes later the arteries were exposed for 2 minutes to potassium depolarizing solution (K^+ replacing Na^+ in PSS, ie, 124 mmol L^{-1}; termed KPSS), before replacing with PSS. Subsequent responses were expressed as a % of this KPSS reference contraction in each artery. Rat or mouse mesenteric arteries that contracted to KPSS with <3 mN force, mouse tail arteries that contracted to KPSS with <20 mN force, or rat and mouse pulmonary arteries that contracted to KPSS with <1 mN force were considered as violations of predetermined criteria. As a further test of viability of the artery, a single 2-minute exposure to 10 μmol L^{-1} noradrenaline was performed and then replaced with drug-free PSS. To test the integrity of the endothelium, arteries were precontracted with noradrenaline

1 μmol L^{-1} (which contracts to about 80% of KPSS) and acetylcholine 1 μmol L^{-1} was added which would normally completely relax the artery in <30 seconds to the baseline force. Some arteries were equilibrated for 30 minutes with L-NAME (N_ω-nitro-L-arginine methyl ester; 100 μmol L^{-1}) and one concentration of an endothelin antagonist (bosentan 1, 10, or 100 μmol L^{-1}; BQ788 0.3, 1, or 3 μmol L^{-1}). In one study, BQ788 3 μmol L^{-1} and 0, 1, or 10 μmol L^{-1} bosentan were equilibrated before the concentration-response curve was constructed to endothelin-1. In each study, the artery was then exposed to a single cumulative concentration-contraction curve (0.1 nmol L^{-1} to 3 μmol L^{-1}, depending on agonist, tissue, and treatment) to either sarafotoxin S6c or endothelin-1, added in half-$\log_{10}$ M increments allowing time for the contraction to reach a plateau before raising the concentration.

2.2 | Endothelium removal

In rat small pulmonary artery, the normalization procedure was completed before testing the relaxation to acetylcholine 1 μmol L^{-1} in arteries contracted by U46619 (0.1 μmol L^{-1}). The artery passive force was then relaxed, and a human black hair was inserted into the artery lumen. Lateral movement of the hair and careful rotation of the artery loosely suspended on the 2 wires removed the endothelial cells. The passive force was reapplied to the level prior to the endothelial cell removal and the acetylcholine (1 μmol L^{-1}) test repeated in the presence of U46619 (0.1 μmol L^{-1}). Failure to relax to acetylcholine was considered the functional test of endothelial cell removal. The endothelium-denuded arteries can still deliver a full relaxation response to sodium nitroprusside 1 μmol L^{-1}.

2.3 | Trachea

The main trachea (10 mm long) was dissected free from the rat, cut into 2- to 3-mm-long ring segments, and mounted on wires in 15-mL organ baths (see figure 1 in Angus and Wright),[15] used for large diameter ring segments. In some trachea ring segments, the epithelial cell layer was removed by using a splinter of wood and gently rubbing the lumen for 1 minute. The rings were stretched to a passive

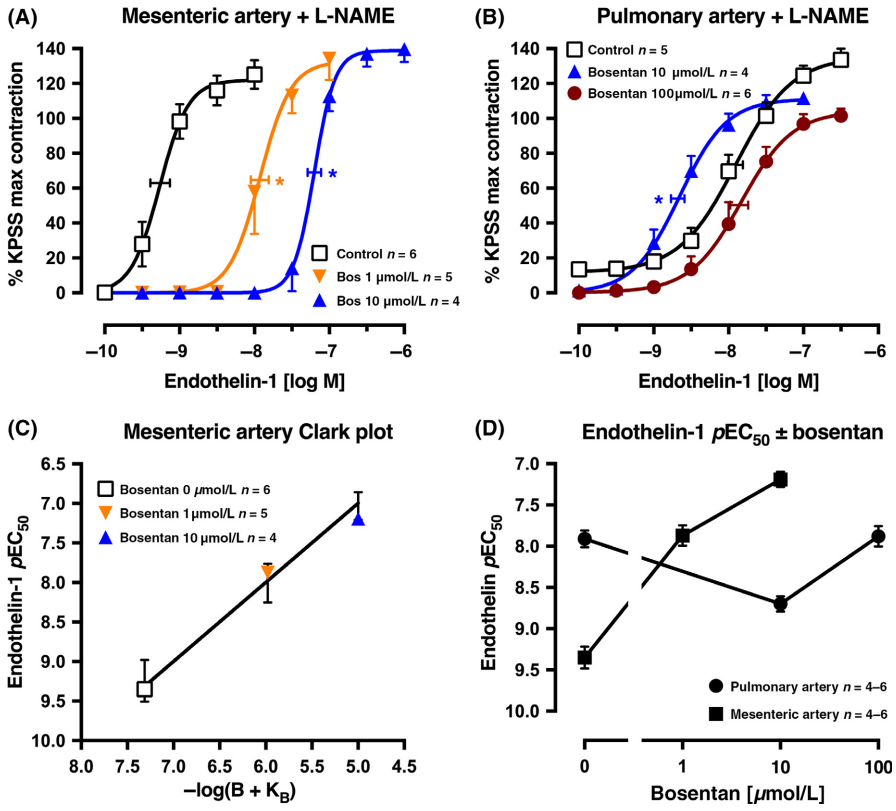

FIGURE 1 Average single exposure concentration-contraction curves to endothelin-1 in rat (A) mesenteric artery (n = 15) and (B) pulmonary artery (n = 15), pretreated with L-NAME 100 μmol L^{-1}, in the absence Control, (0 μmol L^{-1}) or presence of bosentan 1, 10 or 100 μmol L^{-1}. Data are expressed as % KPSS maximum contraction (y axis). (C) Clark plot display for the relationship in the rat mesenteric artery between the endothelin-1 pEC_{50} values (y axis; −log M) and $-\log(B + K_B)$ where B is concentration of bosentan (0, 1, or 10 μmol L^{-1}) and K_B is the global-fitted dissociation constant. The error bars are ± 2 SEM of the difference between the nonlinear regression-fitted pEC_{50} values for endothelin-1 and the pEC_{50} values fitted for the individual artery for each concentration of bosentan (B). (D) The pEC_{50} values for the endothelin-1 curves in (A) and (B) are plotted on the y axis against the bosentan concentration (x axis) for each artery type. Vertical error bars in (A, B, and D) are ± 1 SEM (those not shown are contained within the symbol). Horizontal error bars (A-B) represent the EC_{50} ± 1 SEM. n, number of arteries isolated from separate animals. *$P < .05$, pEC_{50} values compared with respective control (0 μmol L^{-1}) pEC_{50} values. Variations in n are due to violation of predetermined criteria: mesenteric arteries that contracted to KPSS with <3 mN force or pulmonary arteries that contracted to KPSS with <1 mN force

force of 1 g and equilibrated in PSS at 37°C for 60 minutes. A reference contraction to KPSS (62 mmol L^{-1} for trachea, see Clozel et al[17]) was obtained before washing the tissue with drug-free PSS. Subsequent responses were expressed as a % of this KPSS reference contraction in each tracheal ring. Tracheae that contracted to KPSS with <1 g force were considered as violations of predetermined criteria. The resting force was readjusted to 1 g and the trachea left to equilibrate for 30 minutes in the absence or presence of bosentan (3, 10, or 30 μmol L^{-1}). A single concentration-contraction curve to sarafotoxin S6c or endothelin-1 was constructed up to a maximum concentration of 0.3 μmol L^{-1} for sarafotoxin S6c or 3 μmol L^{-1} for endothelin-1.

2.4 | Drugs

Drugs used were acetylcholine bromide (Sigma, St Louis, MO, USA); ambrisentan (Selleckchem, Houston, TX, USA); bosentan sodium salt (Selleckchem); BQ788 sodium salt (Peptides International, Louisville, KY, USA); endothelin-1 (Genscript, Piscataway, NJ, USA); macitentan (Selleckchem); N_ω-nitro-L-arginine methyl ester hydrochloride (Sigma); (-)-noradrenaline bitartrate (Sigma); and sarafotoxin S6c (Auspep, Parkville, Victoria, Australia). All drugs were dissolved in MilliQ water except for endothelin-1 which was dissolved in 10% dimethylformamide to 10^{-4} mol L^{-1}, then diluted in MilliQ water, macitentan which was dissolved in DMSO to 10^{-3} mol L^{-1}, then diluted in MilliQ water, and BQ788 which was dissolved in DMSO to 10^{-4} mol L^{-1}.

2.5 | Statistics and analyses

All data are expressed as mean ± SEM from *n* experiments. The data and analyses comply with the recommendations on experimental design and analysis in pharmacology.[18] All contraction responses to endothelin-1 or sarafotoxin S6c were measured as a % of the Emax (maximum response to agonist) to KPSS within each artery or tracheal ring. Each individual sigmoidal concentration-contraction curve to endothelin-1 or sarafotoxin S6c in the absence or presence of an endothelin receptor antagonist was fitted using Prism 7 (GraphPad Software, La Jolla, CA, USA). The pEC_{50} ± SEM values ($-\log_{10}$ M EC_{50}) were determined for each treatment group. In endothelin-1 experiments in rat trachea, the concentration-contraction curves were not fitted as Emax values were not defined; instead, endothelin-1 pEC_{50} values were calculated at responses of 50% KPSS maximum contraction. pEC_{50} values in treatment groups were compared to the respective control group with a one-way ANOVA and Dunnett's post hoc test (Prism 7). Blinding was not performed for this study as all experiments yielded strict quantitative data.

2.6 | Clark plot and analyses

Endothelin-1 rapidly activates the respective ET_A or ET_B receptors before being internalized for recycling (ET_A) or destruction (ET_B) (see Bremnes et al[19] and Paasche et al[20]). This phenomenon makes it particularly difficult to establish multiple concentration-response curves within a particular artery. In practical terms, the ET_A or ET_B receptor may be rapidly activated, but the resultant calcium mobilization and contraction takes a considerable time to develop even in small arteries <200 μm diameter. Thus, we routinely designed our experiments around a single cumulative concentration-response curve in the presence or absence of an antagonist concentration.

Our chosen experimental design of only one concentration-response curve per tissue does not allow for Schild plot analyses or determination of concentration ratios within tissue. By preference, we used the Clark plot and global fit analysis with its robust advantages.[21] To determine the antagonist dissociation constant (K_B) for each endothelin antagonist, we applied the global regression method[22] that was simplified from that developed originally by Stone and Angus.[21] A computer-based nonlinear regression was performed to solve for K_B ($pK_B = -\log K_B$) by iterative approximation for ALL the endothelin-1 (or sarafotoxin S6c) pEC_{50} values in the absence or presence of antagonist (B) concentrations thus:

$$pEC_{50} = -\log[(B)^n + 10^{-pK}B] - \log c \quad (1)$$

where n is a "power departure" equivalent to allowing the slope of a Schild plot to vary from unity (see Lew and Angus[22]).

Having solved pK_B, the relationship between the mean pEC_{50} values of the actual data were plotted against the antagonist concentration $-\log(B + K_B)$ at concentrations of bosentan (0, 1, 3, 10, 30, or 100 μmol L^{-1}), ambrisentan (0, 1, 3, or 10 μmol L^{-1}), or macitentan (0, 0.3, 1, or 10 μmol L^{-1}). This graphical display was named the Clark plot by Stone and Angus[21] as it was similar to the plot developed by Clark[23] of log(agonist) vs log(antagonist) at equal level of response. There are 2 important ways to test whether the concentration-response curves are displaced to the right of the control pEC_{50} according to simple competitive antagonism. First, whether the 95% confidence limits for n contains 1; if so, the equation 1 is fitted where n = 1. Second, the error bars on the Clark plot are ± 2 times the standard error of the differences between the observed endothelin-1 (or sarafotoxin S6c) pEC_{50} values and the predicted pEC_{50} values from the fitted equation 1. This provides an estimate of the confidence band around the line. If the point showing the average of the observed pEC_{50} values at a level of $-\log(B + K_B)$ fell outside the error bar, this would indicate a departure from the simple competitivity model.

For comparison of pK_B values between each antagonist in different settings, an unpaired Student's *t* test (Prism 7) was performed. Statistical significance was taken when $P < .05$.

3 | RESULTS

3.1 | Rat mesenteric and pulmonary small arteries

In rat small mesenteric arteries (i.d. 352 ± 6 μm), single endothelin-1 concentration-response curves had a pEC_{50} of 8.12 ± 0.02 and an Emax of 108 ± 5% KPSS (n = 4; data not shown). In the presence of L-NAME (100 μmol L^{-1}), the pEC_{50} for endothelin-1 was 9.35 ± 0.13 (n = 6), significantly higher (17-fold more potent) than

in the absence of L-NAME, and the Emax was 123 ± 9% KPSS (Figure 1A). In rat small second-order pulmonary arteries (524 ± 20 μm i.d.), the pEC_{50} for endothelin-1 was 7.55 ± 0.20 with an Emax of 124 ± 4% KPSS (n = 5; data not shown). In the presence of L-NAME (100 μmol L^{-1}), the pEC_{50} was 7.91 ± 0.10, not significantly different from control, and the Emax was 135 ± 7% KPSS (n = 5; Figure 1B). In the presence of L-NAME and bosentan 1 and 10 μmol L^{-1}, the endothelin-1 concentration-response curves were right-shifted in a competitive manner in the rat mesenteric artery (Figure 1A), but significantly left-shifted with bosentan 10 μmol L^{-1} in the rat pulmonary artery (Figure 1B). In the presence of bosentan 100 μmol L^{-1}, the endothelin-1 curve was located not significantly different to the control in the presence of L-NAME (Figure 1B). For the mesenteric artery, the Clark plot and analyses indicate a pK_B of 7.31 ± 0.16 (n = 15 points), congruent with the model of competitive antagonism (Figure 1C). A display of the pEC_{50} values for endothelin-1 concentration-response curves shows the significantly different control pEC_{50} for endothelin-1 in the 2 artery types and the opposite effect on the pEC_{50} by bosentan 10 μmol L^{-1}, all in the presence of L-NAME (Figure 1D). Clearly, the presence of 100 μmol L^{-1} bosentan had very little effect in antagonizing the endothelin-1 contraction when compared with control (0 μmol L^{-1} bosentan) in the pulmonary artery.

The failure to obtain an estimate of the pK_B for bosentan in rat small pulmonary artery, possibly due to the removal of the agonist endothelin-1, prompted the use of the nonendogenous ET_B-selective ligand sarafotoxin S6c in the absence or presence of L-NAME. The control (0 μmol L^{-1} bosentan) curve was more potent (4.1-fold) in the presence of L-NAME (pEC_{50} with L-NAME 9.31 ± 0.09, n = 6, and without L-NAME 8.70 ± 0.19, n = 5; Figure 2A,B), suggesting a small effect of NO release in functionally antagonizing the contraction. The Clark plots and analyses show that bosentan is a competitive antagonist with similar pK_B values in the absence or presence of L-NAME of 5.52 ± 0.17 (n = 15 points) and 5.91 ± 0.24 (n = 17 points), respectively (Figure 2C,D).

The more direct test for the role of ET_B receptors in the endothelial clearance of endothelin-1 was concluded from the interaction of the highly selective ET_B receptor antagonist BQ788 and endothelin-1 in the absence of the endothelium (Figure 3A). Again BQ788 (0.3-3 μmol L^{-1}) appeared to slightly left-shift (potentiate) the endothelin-1 concentration-response curve pEC_{50}. Moreover, this family of curves was similar in pattern to the curves in the presence of L-NAME and endothelium (Figure 3B,E-F), suggesting that ET_B-mediated clearance of endothelin-1 may well be dependent on the smooth muscle cells in this artery rather than on the endothelium. To calibrate the ET_B receptor on smooth muscle in the absence of NO release or clearance, we tested individual concentration-response curves for sarafotoxin S6c with increasing concentrations of BQ788 in the presence of L-NAME (100 μmol L^{-1}) (Figure 3D). The global fit and Clark plot gave a pK_B of 7.20 ± 0.21 (n = 20 points; Figure 3H). In the presence of BQ788 3 μmol L^{-1} to antagonize the ET_B-mediated clearance of endothelin-1 and antagonize the ET_B-mediated contraction, endothelin-1 still contracted the pulmonary artery with a pEC_{50} of 7.05 ± 0.16 indicating that ET_A

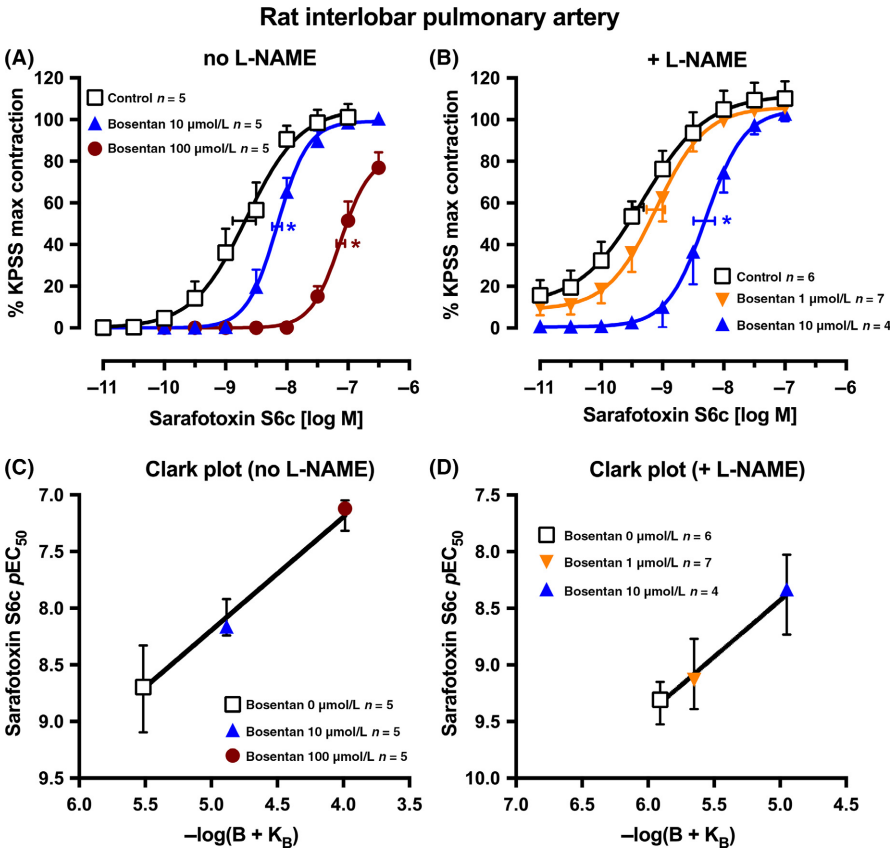

FIGURE 2 Average single exposure concentration-contraction curves to sarafotoxin S6c in rat pulmonary artery in the (A) absence or (B) presence of L-NAME 100 μmol L^{-1} and of bosentan 0 (Control), 1, 10, or 100 μmol L^{-1}. Data are expressed as % KPSS maximum contraction (y axis). Vertical error bars are ± 1 SEM (those not shown are contained within the symbol). Horizontal error bars represent the EC_{50} ± 1 SEM. (C-D) Clark plot displays for the corresponding figure panel above for the relationship between the sarafotoxin S6c pEC_{50} values (y axis; −log M) and −log(B + K_B) values (see legend for Figure 1C) in the absence (C) or presence (D) of L-NAME. n, number of arteries isolated from separate animals. *$P < .05$, pEC_{50} values compared with respective control (0 μmol L^{-1}) pEC_{50} values. Variations in *n* are due to violation of a predetermined criterion: arteries that contracted to KPSS with <1 mN force

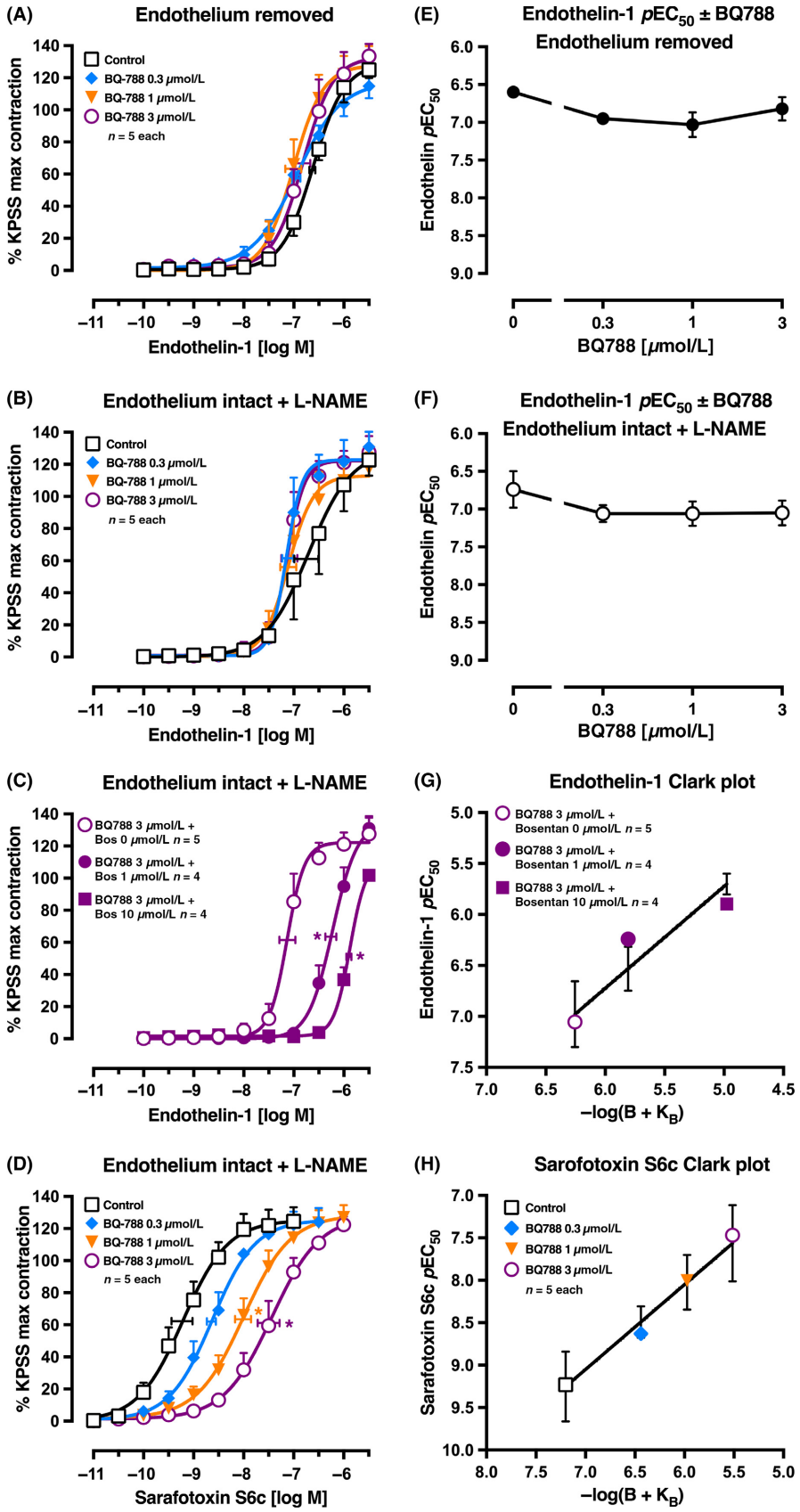

FIGURE 3 Average single exposure concentration-contraction curves to (A-C) endothelin-1 or (D) sarafotoxin S6c in rat pulmonary artery in the (A) absence of endothelium or (B-D) presence of endothelium plus L-NAME 100 μmol L^{-1}. (A, B, and D) Curves were completed in the absence (Control, 0 μmol L^{-1}) or presence of BQ788 0.3, 1, or 3 μmol L^{-1}. (C) Curves were completed in the presence of BQ788 3 μmol L^{-1} plus bosentan 0, 1, or 10 μmol L^{-1}. Data are expressed as % KPSS maximum contraction (y axis). (E-F) The pEC_{50} values from (A-B) are plotted on the y axis against the BQ788 concentration (x axis). Vertical error bars (A-F) are ± 1 SEM (those not shown are contained within the symbol). Horizontal error bars (A-D) represent the EC_{50} ± 1 SEM. (G-H) Clark plot displays for the corresponding left figure panel for the relationship between the (G) endothelin-1 or (H) sarafotoxin S6c pEC_{50} values (y axis; −log M) and $-\log(B + K_B)$ values (see legend for Figure 1C) in the presence of L-NAME. *$P < .05$, pEC_{50} values compared with respective control (0 μmol L^{-1}) pEC_{50} values. *n*, number of arteries isolated from separate animals. Variations in *n* are due to violation of a predetermined criterion: arteries that contracted to KPSS with <1 mN force

receptors were now operating (Figure 3C). To test this, equilibration with bosentan 0, 1, and 10 μmol L^{-1} gave right-shifted concentration-response curves and a pK_B of 6.26 ± 0.23 (n = 13 points; Clark plot, Figure 3G). Note that the Clark plot display indicates that competitivity was not achieved as points lie outside the error bars for bosentan 1 and 10 μmol L^{-1}.

Evidence that L-NAME or endothelial cell removal had abolished the relaxation to acetylcholine 1 μmol L^{-1} was shown by the result that before treatment with L-NAME or endothelial removal the relaxation to acetylcholine 1 μmol L^{-1} as a % of the precontractile tone was −54 ± 4% (n = 19) or −56 ± 2% (n = 18), respectively, and after treatment was −2 ± 2% or −1 ± 2%, respectively (data not shown).

3.2 | Other arteries

In the mouse, we examined 3 different arteries to determine if the responses to bosentan and endothelin-1 in the small pulmonary artery of the rat could be replicated. In the main pulmonary artery (i.d. 648 ± 20 μm), mesenteric artery (i.d. 275 ± 15 μm), and tail artery (i.d. 370 ± 6 μm), the patterns of endothelin-1 concentration-response curves and antagonism by bosentan were similar (Figure 4A-C). The Clark plots and analyses showed pK_B values for bosentan of 7.16 ± 0.13 (n = 17 points), 6.24 ± 0.16 (n = 14 points), and 6.52 ± 0.18 (n = 17 points) in the pulmonary, mesenteric, and tail arteries, respectively, and complied with the model of simple competitivity (Figure 4D-F).

3.3 | Macitentan

In the rat small mesenteric artery, macitentan (0.3 and 1 μmol L^{-1}) was a potent competitive endothelin-1 receptor antagonist (Figure 5A). The Clark plot and analyses gave a pK_B of 7.05 ± 0.10 (n = 15 points) and fitted the competitive model. The endothelin-1 concentration-contraction curves in the rat small pulmonary artery were completely unaffected by 1 and 10 μmol L^{-1} macitentan, as shown in Figure 5B.

3.4 | Ambrisentan

In the rat small mesenteric artery, ambrisentan (1 and 3 μmol L^{-1}) was a potent competitive endothelin-1 receptor antagonist (Figure 5C). The Clark plot and analyses gave a pK_B of 6.60 ± 0.07 (n = 13 points) and fitted the competitive model. In contrast, endothelin-1 concentration-contraction curves in the rat small pulmonary artery were slightly left-shifted from control by ambrisentan 1 μmol L^{-1} before showing a small right-shift at 10 μmol L^{-1} (Figure 5D).

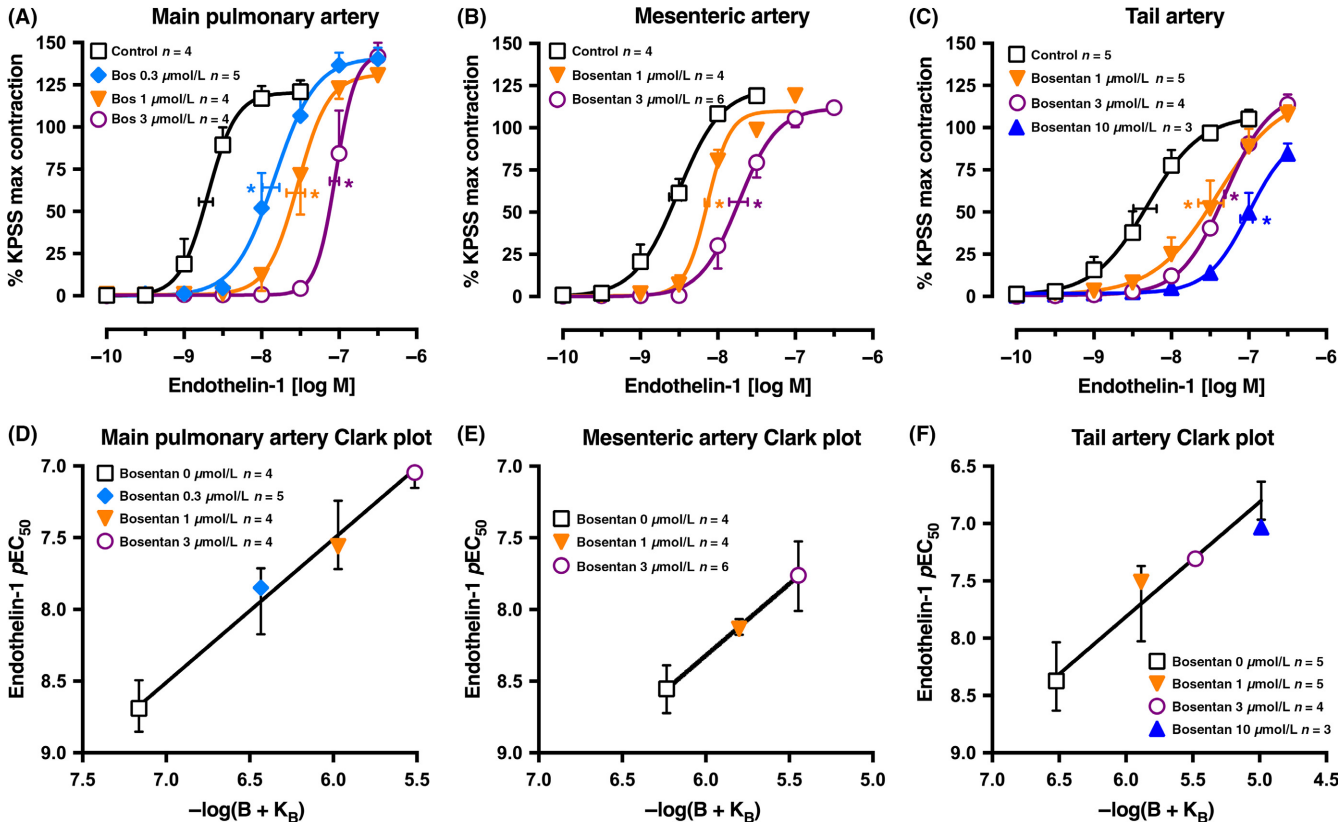

FIGURE 4 Average single exposure concentration-contraction curves to endothelin-1 in Swiss mouse isolated (A) main pulmonary, (B) mesenteric, and (C) tail arteries in the absence and presence of bosentan (0 (Control), 0.3, 1, 3, or 10 μmol L^{-1}). Data are expressed as % KPSS maximum contraction (y axis). Vertical error bars are ± 1 SEM (those not shown are contained within the symbol). Horizontal error bars represent the EC_{50} ± 1 SEM. (D-F) Clark plot displays for the corresponding figure panel above for the relationship between the endothelin-1 pEC_{50} values (y axis; −log M) and −log(B + K_B) values (see legend for Figure 1C). *n*, number of arteries isolated from separate animals. *$P < .05$, pEC_{50} values compared with respective control (0 μmol L^{-1}) pEC_{50} values. Variations in *n* are due to violation of predetermined criteria: pulmonary arteries that contracted to KPSS with <1 mN force; mesenteric arteries that contracted to KPSS with <3 mN force; or tail arteries that contracted to KPSS with <20 mN force

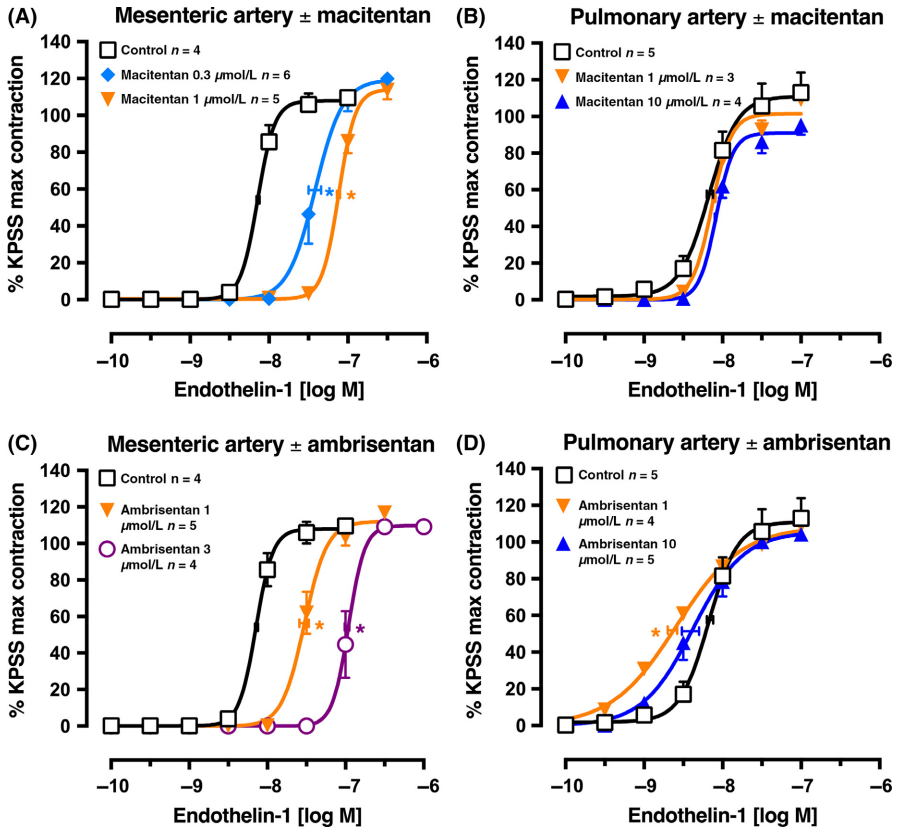

FIGURE 5 Average single exposure concentration-contraction curves to endothelin-1 in rat (A) and (C) mesenteric artery (n = 13-15) or (B) and (D) pulmonary artery (n = 12-14) in the absence (Control, 0 μmol L^{-1}) or presence of (A-B) macitentan 0.3, 1, or 10 μmol L^{-1} or (C-D) ambrisentan 1, 3, or 10 μmol L^{-1}. Data are expressed as % KPSS maximum contraction (y axis). Vertical error bars are ± 1 SEM (those not shown are contained within the symbol). Horizontal error bars represent the EC_{50} ± 1 SEM. *P < .05, pEC_{50} values compared with respective control (0 μmol L^{-1}) pEC_{50} values. Variations in n are due to violation of predetermined criteria: mesenteric arteries that contracted to KPSS with <3 mN force or pulmonary arteries that contracted to KPSS with <1 mN force

3.5 | Rat trachea

As was observed in rat small pulmonary artery, sarafotoxin S6c was significantly more potent than endothelin-1 in contracting the rat isolated trachea with the epithelium intact in the absence of any antagonist (pEC_{50} values: sarafotoxin S6c 8.72 ± 0.22, n = 4; endothelin-1 6.82 ± 0.09, n = 7; Figure 6A,B). In the absence of epithelium, the pEC_{50} for sarafotoxin S6c was not changed (8.63 ± 0.13, n = 5) and similarly for endothelin-1 (6.61 ± 0.17, n = 4) (Figure 6C,D). The low potency of endothelin-1 in rat trachea prevented exploration of the full concentration-response curve, and therefore, we calculated pEC_{50} values at responses of 50% KPSS maximum contraction. In contrast, the full sarafotoxin S6c concentration-response curves were obtained to allow pEC_{50} values to be calculated from logistic curve analysis, often when the Emax was more than 100% KPSS.

Bosentan (3-30 μmol L^{-1}) right-shifted the endothelin-1 and sarafotoxin S6c concentration-contraction curves. The Clark plot and analysis show that with sarafotoxin S6c and epithelium intact, bosentan's pK_B was 5.76 ± 0.23 (n = 20 points), not significantly different from endothelin-1 as agonist with a pK_B of 5.41 ± 0.28 (n = 28 points; Figure 6E,F). In epithelium-denuded trachea, with sarafotoxin S6c, the bosentan pK_B was 6.06 ± 0.18 (n = 20 points), significantly higher than for endothelin-1 as agonist (pK_B 5.02 ± 0.31, n = 17 points).

3.6 | Modeling

To model the interaction between endothelin-1 clearance and ET_B and ET_A receptor antagonism of the contraction response in small pulmonary arteries, we set the following criteria:

1. The ET_B receptor-sensitive endothelin-1 clearance mechanism (C_{ETB}) can decrease the endothelin-1 concentration at the ET_A or ET_B receptor environment by a maximum of 10-fold (1 pEC_{50} unit).
2. The theoretical dual ET_A and ET_B receptor antagonist has the same pK_B value (8.5) at the "clearance ET_B receptor" as at the ET_B and ET_A receptor modulating contraction.
3. The efficiency of endothelin-1 at ET_A and ET_B constrictor receptors is the same.

In Figure 7A, we set the control pEC_{50} for the sarafotoxin S6c concentration-response curve at 8.8 so that a twofold shift (log 0.3) would result in a pEC_{50} of 8.5 in the presence of an ET_A and ET_B antagonist with a pK_B of 8.5 (3 nmol L^{-1}). Similarly, we set the control pEC_{50} for endothelin-1 at 7.8. Assuming that the ET_B (sarafotoxin S6c) assay was not compromised by clearance nor the endothelin-1 assay (like mesenteric artery or rat aorta), then the pEC_{50} in the presence of the dual ET receptor antagonist (8.5-6.5 −log M) would rise as shown in Figure 7A and the Schild plot would show competitive antagonism (slope = 1) and pK_B 8.5 (Figure 7B). If

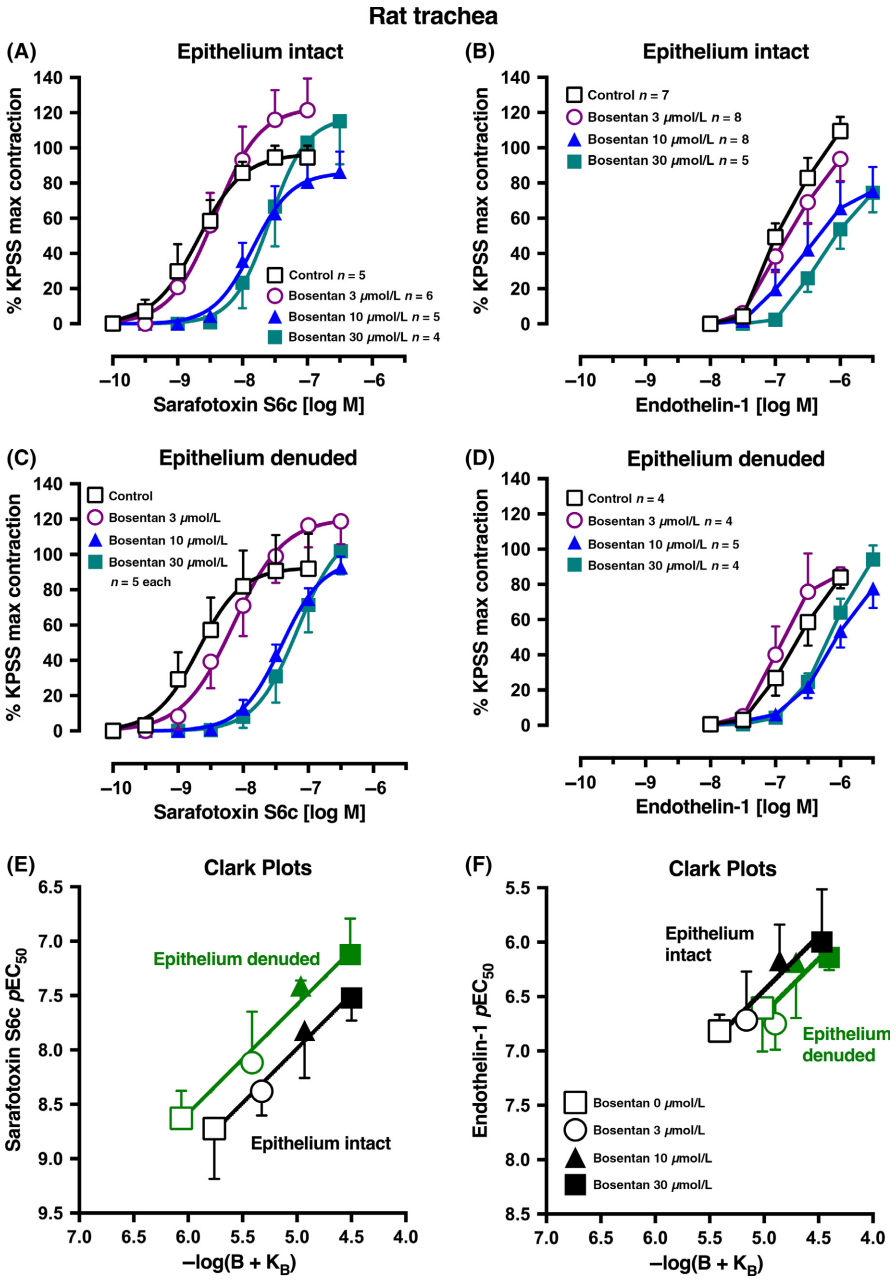

FIGURE 6 Average single concentration-contraction curves to (A) sarafotoxin S6c or (B) endothelin-1 in rat isolated trachea with intact epithelium in the absence (Control, 0 μmol L^{-1}) or presence of bosentan 3, 10, or 30 μmol L^{-1}. (C-D) Corresponding agonist curves in trachea with epithelium denuded. Data are expressed as % KPSS maximum contraction (y axis). Error bars in (A-D) are ± 1 SEM (those not shown are contained within the symbol). (E-F) Clark plot displays for the relationship in the rat trachea between the (E) sarafotoxin S6c or (F) endothelin-1 pEC_{50} values (y axis; −log M) and −log(B + K_B) where B is concentration of bosentan (0, 3, 10, or 30 μmol L^{-1}) and K_B is the global-fitted dissociation constant (see legend for Figure 1C). n, number of tracheal rings isolated from separate animals. Variations in *n* are due to violation of a predetermined criterion: tracheae that contracted to KPSS with <1 g force

the assay is of predominantly ET_B receptors and the clearance mechanism is active, as we hypothesize in the small pulmonary artery, the control pEC_{50} for endothelin-1 would lower to 6.8 as endothelin-1 is removed from the receptor locus by the clearance mechanism (Figure 7A; ●). In the presence of the dual ET_A and ET_B antagonist, endothelin-1 would be both potentiated in concentration available to ET_B receptors as the clearance mechanism is antagonized, but in addition, the endothelin-1 concentration would be inhibited at the ET_B receptor mediating contraction. This is shown graphically in Figure 7A where at 3 concentrations of the dual antagonist, the endothelin-1 pEC_{50} is both enhanced (●) and antagonized (▲) with 8.5, 8, 7.5, 7, and 6.5 −log M. To the experimenter of course, only the resultant of the potentiation and antagonism might be observed as shown by the ▲ flat line until surmountable antagonism is observed at 7 (–log M).

The relationship between the endothelin-1 pEC_{50} and the ET_A and ET_B receptor antagonist concentrations is best illustrated in a Schild plot (Figure 7B). The dual ET_A and ET_B antagonist in the absence of the ET_B clearance mechanism shows slope 1 and pK_B 8.5 for the agonists endothelin-1 at an ET_A receptor-only assay and pK_B 8.5 for sarafotoxin S6c at an ET_B receptor assay. Note that at *p*Antagonist 6.5, the ET_A and ET_B shift is 100-fold (log(concentration ratio − 1) = 2). But if the endothelin-1 clearance mechanism is active, as in small pulmonary arteries, the shift at constrictor ET_B receptors is now only 10-fold at *p*Antagonist 6.5 as the pK_B has moved to 7.5. Clinically, this scenario would demand at least a plasma level of endothelin antagonist of *p*6.5 (ie, 0.3 μmol L^{-1}) if the pK_B at ET_A and ET_B receptors was 8.5.

Two further scenarios have been modeled. First, if the ET_A to ET_B selectivity ratio was ET_A-selective by 30-fold, ie, pK_B for the

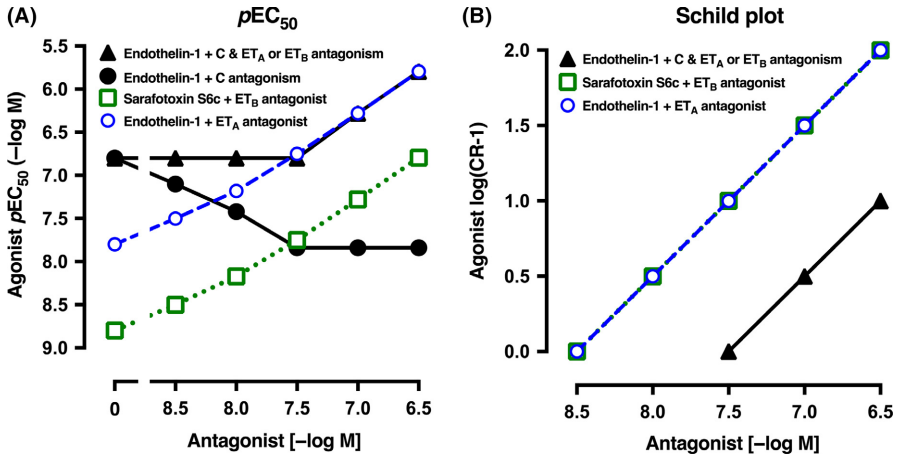

FIGURE 7 (A) Hypothetical relationship between the pEC_{50} values for endothelin-1 or sarafotoxin S6c concentration-contraction curves and the concentration of a theoretical dual ET_A and ET_B receptor antagonist with a pK_B of 8.5 at both receptors. For simplicity, the control (0 antagonist) pEC_{50} for sarafotoxin S6c (□) was set 1 log unit higher (10-fold more potent) than for endothelin-1 (○). In the presence of ET_B receptors and the clearance (C) mechanism for endothelin-1, the maximum clearance was set at 10-fold (1 log unit) so that the pEC_{50} in the presence of no antagonist (0) rises 1 log unit (● or ▲). As the ET_B antagonism starts to block the endothelin-1 clearance, so the pEC_{50} rises (●) but just as does the ET_B and ET_A antagonism so that the resultant shows the actual pEC_{50} is not altered. (B) The Schild plot for endothelin-1 (or sarafotoxin S6c) as the agonist and the dual ET_A and ET_B antagonist with pK_B of 8.5 is shown. Separate theoretical lines are shown for ET_A (○; eg, rat aorta) and ET_B (□; eg, trachea). In the presence of ET_B-mediated clearance (C) that removes endothelin-1, as in pulmonary artery, the Schild plot points (▲) move parallel 1 log unit to decrease the potency of the dual antagonist by 10-fold (ie, the pK_B of 8.5 becomes 7.5). The y axis is the agonist log(concentration ratio–1) and the x axis shows the concentration of dual ET_A and ET_B antagonist (−log M)

ET antagonist at ET_A receptors was 8.5 and 7.0 for ET_B receptors, the Schild plot with endothelin-1 clearance active shows that to reach a 10-fold antagonism at ET_B constrictor receptors, then the plasma concentration would need to reach 10 μmol L^{-1} (*p*5 mol L^{-1}), and at this concentration, the antagonism of ET_A receptors would be 3000-fold (Figure 8A). The second scenario is when an endothelin antagonist has a 10-fold selectivity for ET_B over ET_A receptors; thus, pK_B at ET_B receptors is set at 8.5 and for ET_A receptors at 7.5. The Schild plot (Figure 8B) shows that endothelin-1 clearance will effectively decrease the pK_B of antagonism at ET_B constrictor receptors to 7.5, the same as ET_A. Thus, a concentration of 0.3 μmol L^{-1} would result in a 10-fold shift in both ET_A and ET_B receptors in the presence of endothelin-1 clearance.

We also present the Schild plot for compound A-182086 which was developed with just threefold ET_A to ET_B selectivity (pK_B at ET_A 8.5 and at ET_B 8; Figure 8C). Thus, in the presence of clearance, the plasma levels would need to be about 1 μmol L^{-1} (ie, 6 −log M) for a 10-fold shift in ET_B receptor constrictor activity, while there would be at least 300-fold shift for ET_A receptors. Indeed, these peak plasma levels of 4.3 μmol L^{-1} were achieved in rats given A-182086 10 mg·kg^{-1} oral or even greater in dogs (34.5 μmol L^{-1}), but significantly less in monkeys (0.16 μmol L^{-1}) as the bioavailability varied from 54%, 71%, and 11%, respectively.[24]

Finally, we present the theoretical Schild plot for a selective ET_B antagonist Ro 46-8443 where the pK_B at ET_B is 7.1 and 5.7 at ET_A receptors (Figure 8D). This ET_B to ET_A selectivity of 25 shows an important effect that when even with clearance in operation there is still more ET_B constrictor antagonism than ET_A.

4 | DISCUSSION

Our work supports the hypothesis that in very specific vascular beds, the local clearance of endothelin-1 lowers the endothelin-1 concentration that would activate ET_A or ET_B endothelin receptors. The pK_B estimate for ET_A, ET_B, or mixed ET_A and ET_B receptor antagonists will be confounded by 2 competing processes: one to potentiate the agonist endothelin-1 and the second to antagonize its action at ET_A and/or ET_B receptors.

The tissue assays reported here confirm that there are special defined locations in some vascular beds and tracheal tissue that have a major population of ET_B receptors on smooth muscle. Functional ET_B receptors were defined by the substantial contraction up to the tissue maximum by the potent ET_B-selective agonist sarafotoxin S6c. This agonist is not a substrate for the ET_B receptor-sensitive clearance mechanism specifically shown for endothelin-1 and blocked by ET_B antagonists. Thus, the rat tracheal ring with agonist sarafotoxin S6c and epithelium intact proved to be a robust assay to define the pK_B for ET_B antagonists. We calculated the pK_B for bosentan as 5.76 ± 0.23 for ET_B receptors with sarafotoxin S6c and similarly 5.41 ± 0.28 with endothelin-1. Importantly, the pK_B for bosentan and sarafotoxin S6c was the same whether the epithelium was present or absent (pK_B 5.76 ± 0.23 and 6.06 ± 0.18, respectively). In the original bosentan report, in rat tracheal rings, the pA_2 was reported as 5.94 ± 0.04 with Schild slope 0.90 ± 0.18.[17] Thus, tracheal smooth muscle ET_B receptors mediate contraction, but there is no evidence of clearance of endothelin-1 in this assay.

For the ET_A receptor, the analysis is less certain as there is no selective ET_A receptor agonist.[25] The main assay used to determine

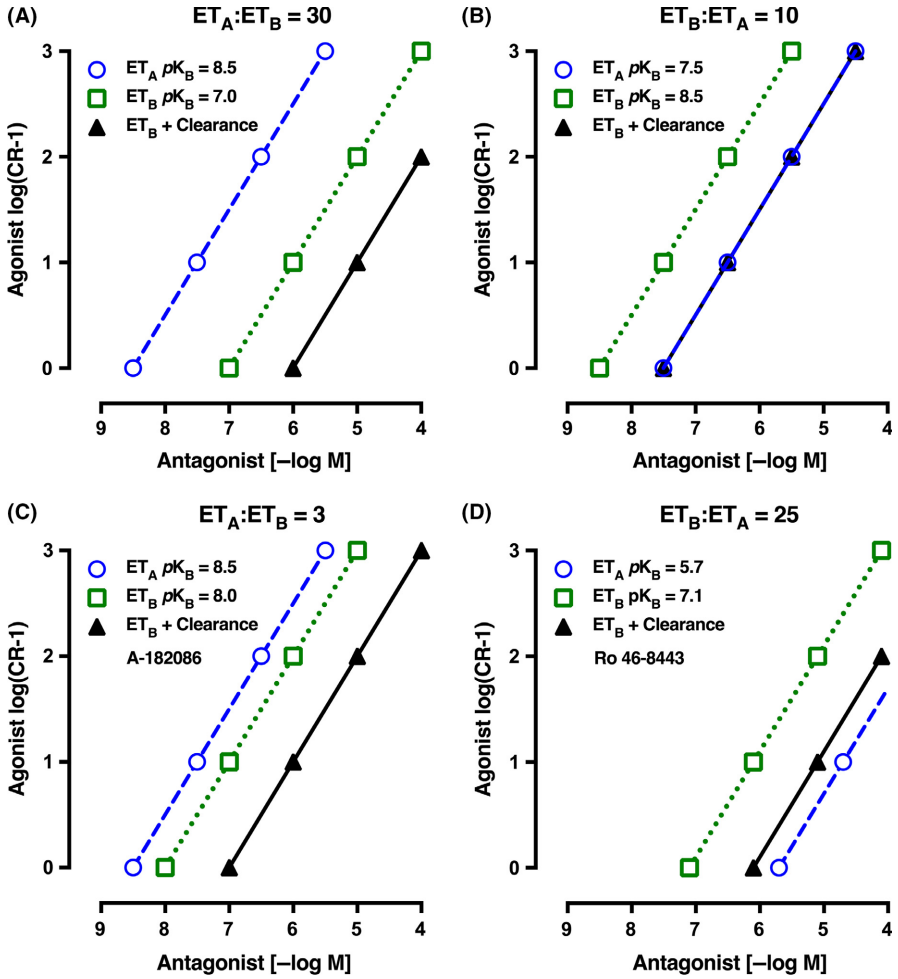

FIGURE 8 (A) Schild plot for a theoretical endothelin-1 antagonist that is 30-fold more selective at ET_A vs ET_B receptors (pK_B: ET_A 8.5 and ET_B 7.0). Note that in the presence of ET_B-mediated clearance, the plasma concentration of the dual antagonist must rise to 10 μmol L^{-1} to give a 10-fold antagonism at ET_B constrictor receptors and 3000-fold antagonism at ET_A constrictor receptors. (B) Schild plot for a theoretical endothelin-1 antagonist that is 10-fold more selective at ET_B vs ET_A receptors (pK_B: ET_B 8.5 and ET_A 7.5). In the presence of ET_B-mediated clearance, the plasma concentration of the dual antagonist must rise to 0.3 μmol L^{-1} to give a 10-fold antagonism at both ET_B and ET_A receptors. (C) Schild plot for endothelin-1 antagonist A-182086 that is threefold more selective for ET_A vs ET_B receptors (pK_B: ET_A 8.5 and ET_B 8.0; see Table 1). In the presence of ET_B-mediated clearance, the plasma concentration of the dual antagonist must rise to 1 μmol L^{-1} to give a 10-fold antagonism at ET_B constrictor receptors and 300-fold antagonism at ET_A constrictor receptors. (D) Schild plot for endothelin-1 antagonist Ro 46-8443 that is 25-fold more selective at ET_B vs ET_A receptors (pK_B: ET_B 7.1 and ET_A 5.7; see Table 1). In the presence of ET_B-mediated clearance, the plasma concentration of the dual antagonist must rise to 7.9 μmol L^{-1} to give a 10-fold antagonism at ET_B receptors, with a fivefold antagonism at ET_A receptors. The y axis is the agonist log(concentration ratio–1) and the x axis shows the concentration of dual ET_A and ET_B antagonist (−log M)

the pK_B (7.28) for bosentan at ET_A receptors was the contraction to endothelin-1 of rat aortic rings, with endothelium removed.[26] Our competitive pK_B values for bosentan and endothelin-1 in human large diameter arteries such as pulmonary (i.d. 5.5 mm) and radial (i.d. 3.23 mm) [27] and in rat mesenteric small artery (i.d. 0.25 mm) or mouse main pulmonary (i.d. 0.65 mm), mesenteric (i.d. 0.28 mm), and tail (i.d. 0.37 mm) arteries all fall in the range 6.04-7.31, consistent with ET_A receptor antagonism. The one outstanding artery, of those we tested, where the dual ET_A and ET_B antagonist bosentan was apparently very weak was the rat small pulmonary artery.

There are 3 possible factors that could affect the pK_B estimation: (i) endothelin-1 could activate endothelial ET_B receptors to release nitric oxide to functionally antagonize the contraction through smooth muscle cell ET_A or ET_B receptors; (ii) in some arteries, there may be a mix of ET_A and ET_B receptors; and (iii) the ET_B receptor-mediated clearance mechanism has an important action to decrease endothelin-1 local concentrations by as much as 10-fold.

First to the role of nitric oxide, L-NAME made no significant difference to the pK_B estimation for bosentan in rat small pulmonary artery (Figure 2). L-NAME (100 μmol L^{-1}) was effective in eliminating the release of NO as demonstrated by the complete abolition of the relaxation to acetylcholine (1 μmol L^{-1}) in U46619-precontracted arteries. Second, despite L-NAME being present, endothelin-1 was much less potent (lower pEC_{50}) in rat pulmonary small artery than in rat mesenteric artery. Third, in the presence of bosentan 10 μmol L^{-1}, the pEC_{50} for endothelin-1 was right-shifted and

lowered to 7.2 (−log M) in the mesenteric artery, while in contrast, it was left-shifted and raised to a pEC_{50} of 8.7 compared with control in the pulmonary artery (Figure 1A,B). We suggest that this anomalous result and inability to determine a pK_B with bosentan in rat pulmonary artery is explained by the continuous removal of endothelin-1 by the ET_B receptor-sensitive clearance mechanism found in this particular artery, but not in the rat mesenteric artery or aorta, nor human large pulmonary or radial artery.[27]

Further, direct functional evidence of the clearance of endothelin-1 in rat pulmonary artery comes from the selective ET_B antagonist BQ788 assay. With the agonist sarafotoxin S6c, and L-NAME present, the pattern of BQ788 competitive antagonism shows right-shifted concentration-response curves with a pK_B of 7.2 ± 0.21 from Clark plot analysis (Figure 3D,H). In stark contrast, when endothelin-1 was the agonist, BQ788 up to 3 μmol L^{-1} caused no significant rightward shift, if anything a small left-shift indicative of blockade of endothelin-1 ET_B clearance (Figure 3B,F). Removal of the endothelium failed to change the pattern of the endothelin-1 and BQ788 interaction (Figure 3A,E). But bosentan was close to being a competitive ET_A antagonist in the pulmonary artery in the presence of L-NAME *AND* BQ788 to antagonize the clearance of endothelin-1 (Figure 3C,G). Similarly, in human pulmonary resistance arteries, the ET_A receptor antagonist BMS182874 was ineffective against low concentrations of endothelin-1.[28] The finding that endothelium removal did not affect the EC_{50} nor Emax to endothelin-1 or change the action of BQ788 in the rat small pulmonary artery compared to endothelium-intact tissues suggests that the arterial smooth muscle cells are the primary location of the proposed clearance mechanism (Figure 9).

In earlier work, Hay et al[29] reported that in rabbit pulmonary artery, sarafotoxin S6c gave a pK_B of 7.7 for the mixed ET_A and ET_B receptor antagonist SB209670, but 6.7 when endothelin-1 was the agonist. In human small pulmonary arteries (150-200 μm i.d.) sarafotoxin S6c was more than 100-fold more potent than endothelin-1 and the authors concluded that both ET_A and ET_B receptor antagonists are required to antagonize endothelin-1.[28] We also found that the apparently weak antagonism of endothelin-1 by bosentan in rat pulmonary arteries is shared with ambrisentan and macitentan (Figure 5). Indeed, these latter 2 endothelin-1 antagonists are more ET_A than ET_B receptor selective (Table 1). However, it is important to note that the active metabolite of macitentan ACT-132577 may additionally play a significant role as a dual ET_A/ET_B antagonist in vivo. Other factors such as pharmacokinetic differences will also affect the translation of these isolated tissue assay results into the clinic. Thus, there are a number of species including man, rabbit, and rat where small interlobar pulmonary arteries potentially have the

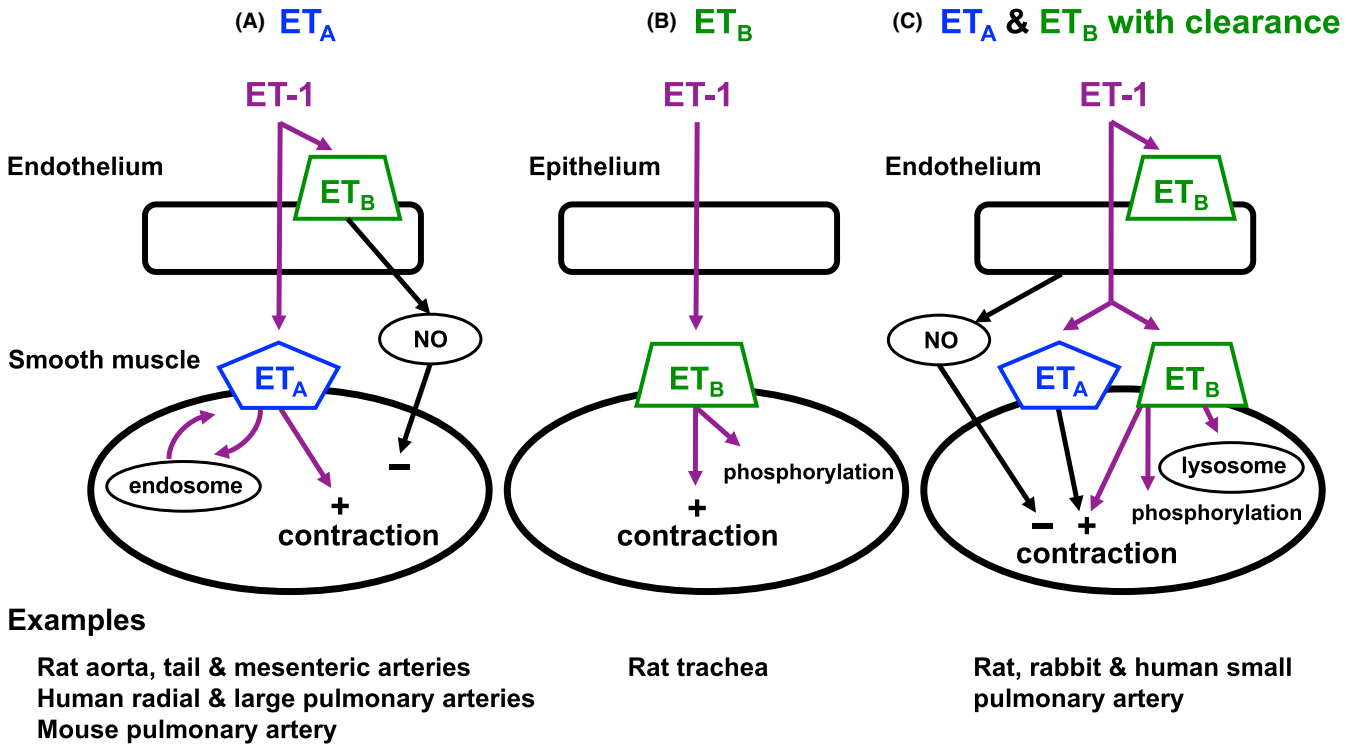

FIGURE 9 Schematic diagram of the location and function of ET_A and ET_B receptors in 3 tissue assays. (A) ET_A receptors located on vascular smooth muscle mediate contraction. ET_A receptors are internalized and recycled slowly through endosomes.[36] (B) ET_B receptors located on smooth muscle cells mediate contraction and are rapidly removed by phosphorylation.[36] (C) ET_B receptors located on smooth muscle cells bind endothelin-1 and clear endothelin-1 from the environment through lysosomal metabolism. The remaining endothelin-1 binds to ET_A and ET_B receptors on smooth muscle to mediate contraction before being recycled by endosomes or destroyed by phosphorylation, respectively. In (A) and (C), ET_B receptors on the endothelium mediate release of NO that transiently relaxes smooth muscle. Examples of the species and tissues assumed to have these particular receptor profiles are given below each panel. ET-1, endothelin-1. NO, nitric oxide

ET_B-sensitive endothelin-1 clearance mechanism and significant populations of ET_B and ET_A receptors on the smooth muscle mediating contraction.

4.1 | Potential clinical implications

We have analyzed the endothelin receptor pharmacology in a wide range of arteries and the small pulmonary artery appears to be unique with its mix of ET_A and ET_B receptors and clearance mechanism. If this finding can be extrapolated to the clinic, there are a number of caveats that must be considered. (i) There is evidence in rats with monocrotaline-induced pulmonary hypertension that the ET_B receptor mRNA and protein expression in small pulmonary arteries are down-regulated.[30] However, in patients with severe pulmonary artery hypertension, the ET_B receptor mRNA and protein expression were upregulated in the media of pulmonary arteries, while the ET_A receptor gene expression was unaffected.[31] (ii) That ET_B receptors on endothelial cells are protective in limiting vascular remodeling and development of pulmonary hypertension, so that ET_B antagonism may well be deleterious.[32] (iii) That pharmacokinetic actions and active metabolites together with protein binding will significantly alter the resultant activity of endothelin receptor antagonists.

Noting the above, there are 3 dual endothelin antagonists approved for pulmonary artery hypertension. On isolated tissue assay data, all have a significant ET_A to ET_B receptor selectivity ratio of 25-50 (Table 1). Our theoretical modeling which reflects our in vitro experimental data (Figures 1 and 8A) suggests that to obtain a 10-fold antagonism of the ET_B constrictor receptor in the presence of clearance, then a plasma concentration of 3000 times higher than the pK_B at ET_A receptors would be required. For bosentan, for example, plasma levels would need to be in the range of 200 μmol L^{-1}! If these levels are not obtained, the antagonist would generally behave only as an effective ET_A antagonist in the clinic.

TABLE 1 Estimates of pK_B from functional isolated tissue assays and selectivity ratios for dual ET_A and ET_B receptor antagonists in the absence or presence of endothelin-1 clearance

	Receptor assay pK_B			Ratio	
Endothelin antagonist	ET_A Aorta[g,h]	ET_B Trachea[g,i]	ET_B + C[j]	ET_A :ET_B[k]	ET_A:ET_B + C[l]
Bosentan[a]	7.3	5.9	4.9	25	250
Ambrisentan[b]	7.1	5.6	4.6	32	320
Macitentan[c]	7.6	5.9	4.9	50	500
A-182086[d]	8.5[m]	8.0[n]	7.0	3	30
Ro 46-8443[e]	5.7	7.1	6.1	0.04	0.4
"Ideal"[f]	8.5	8.5	7.5	1	10

[a]Clozel et al.[17]
[b]Bolli et al.[33]
[c]Iglarz et al.[34]
[d]Wessale et al.[24]
[e]Breu et al.[35]
[f]"Theoretical dualist."
[g]pK_B from Schild plots.
[h]Rat aorta (without endothelium) and agonist endothelin-1.
[i]Rat trachea (without epithelium) and agonist sarafotoxin S6c.
[j]pK_B for ET_B receptors under the influence of endothelin-1 clearance theoretically taken to be 10-fold (ie, 1 log unit).
[k]ET_A to ET_B selectivity ratio calculated as antilog (pK_B ET_A − pK_B ET_B).
[l]ET_A to ET_B + C selectivity ratio calculated as antilog (pK_B ET_A − pK_B ET_B + C).
[m]With endothelium.
[n]Rabbit pulmonary artery (without endothelium).

Our modeling suggests that a 10-fold selective ET_B vs ET_A antagonist might be ideal in antagonizing the pulmonary artery ET_B receptors in the presence of CLEARANCE (Figure 8B). Ro 46-8443[35] is 25-fold selective for ET_B vs ET_A, and modeling would suggest that with a pK_B of 7.1 at ET_B receptors (Figure 8D), a plasma level would be required of nearly 10 μmol L^{-1} to give a 10-fold antagonism of ET_B receptors, but ET_A antagonism would not be sufficient if inhibition of clearance presented a higher level of endothelin-1. Another nonselective and potent ET_A and ET_B antagonist with selectivity ratio of just 3, A-182086 (Table 1), has been used in animals and shows that effective ET_A and ET_B receptor antagonism was achieved after oral dosing.[24]

Given that any antagonism of clearance will raise plasma endothelin-1 levels, there must be sufficient ET_A receptor antagonism present to obviate vasoconstriction from this raised endothelin-1 concentration. Theoretically then, an ET_A vs ET_B selectivity of 10-fold would be sufficient, provided a high plasma concentration is achieved for ET_B antagonism. From Table 1, we predict that given clearance of endothelin-1 in important tissues such as pulmonary artery, the effective ET_B antagonism is 10-fold weaker so that the ET_A to ET_B + clearance selectivity ratio increases by 10-fold. In effect, this suggests that the 3 antagonists in the clinic for pulmonary artery hypertension are principally ET_A-selective agents. The "ideal" antagonist would have identical pK_B values at ET_A and ET_B receptors.

5 | CONCLUSION

This experimental work in isolated tissue assays offers an explanation for the mechanism of the failure of "dual" ET_A and ET_B antagonists to competitively antagonize endothelin-1 in some important arteries such as the small pulmonary artery where ET_A and ET_B receptors predominate to cause contraction. The experimental results and theoretical modeling are consistent with an endothelin-1 clearance mechanism through internalization of endothelin-1 bound to ET_B receptors on smooth muscle of some blood vessels that can lower the endothelin-1 concentration by 10-fold. When this mechanism is blocked by ET_B antagonists, the endothelin-1 concentration will rise. The combination of a possible endothelin-1 clearance and contraction mediated by ET_A and ET_B receptors provides an environment that would prevent effective endothelin-1 receptor antagonism. This conclusion may have important implications for the effective use of endothelin antagonists in the treatment of pulmonary artery hypertension.

ACKNOWLEDGEMENTS

We thank Mr Mark Ross-Smith for expert technical support in isolated artery wire myography and isolated trachea studies. We thank the reviewers for their helpful suggestions which improved our work.

AUTHORS' CONTRIBUTIONS

J.A.A. and C.E.W. conceived the study and designed the protocol. R.J.A.H. performed wire myography studies. J.A.A., C.E.W., and R.J.A.H. collected and analyzed data. J.A.A. and C.E.W. wrote the manuscript. R.J.A.H. critically reviewed the manuscript. All authors approved the final version of the manuscript.

DISCLOSURES

None declared.

ORCID

James A. Angus http://orcid.org/0000-0002-0605-9682
Christine E. Wright http://orcid.org/0000-0002-3339-040X

REFERENCES

1. Fukuroda T, Fujikawa T, Ozaki S, Ishikawa K, Yano M, Nishikibe M. Clearance of circulating endothelin-1 by ET_B receptors in rats. *Biochem Biophys Res Commun*. 1994;199:1461-1465.
2. Gratton JP, Cournoyer G, Loffler BM, Sirois P, D'Orleans-Juste P. ET_B receptor and nitric oxide synthase blockade induce BQ-123-sensitive pressor effects in the rabbit. *Hypertension*. 1997;30:1204-1209.
3. Reinhart GA, Preusser LC, Burke SE, et al. Hypertension induced by blockade of ET_B receptors in conscious nonhuman primates: role of ET_A receptors. *Am J Physiol Heart Circ Physiol*. 2002;283:H1555-H1561.
4. Opgenorth TJ, Wessale JL, Dixon DB, et al. Effects of endothelin receptor antagonists on the plasma immunoreactive endothelin-1 level. *J Cardiovasc Pharmacol*. 2000;36:S292-S296.
5. Johnstrom P, Fryer TD, Richards HK, et al. Positron emission tomography using 18F-labelled endothelin-1 reveals prevention of binding to cardiac receptors owing to tissue-specific clearance by ET B receptors in vivo. *Br J Pharmacol*. 2005;144:115-122.
6. Angus JA, Black JW. Analysis of anomalous pK_B values for metiamide and atropine in the isolated stomach of the mouse. *Br J Pharmacol*. 1979;67:59-65.
7. Kenakin TP. *Pharmacologic analysis of drug-receptor interaction*, 2nd edn. New York: Raven Press; 1993:305-310.
8. Angus JA, Wright CE. Endothelin and the sympathetic nervous system. In: Clozel M, Rubin LJ, eds. *The Endothelin System in Cardiopulmonary Diseases*. Basel: Friedrich Reinhardt Verlag; 2004:97-125.
9. Allcock GH, Warner TD, Vane JR. Roles of endothelin receptors in the regional and systemic vascular responses to ET-1 in the anaesthetized ganglion-blocked rat: use of selective antagonists. *Br J Pharmacol*. 1995;116:2482-2486.
10. D'Orléans-Juste P, Claing A, Télémaque S, Maurice MC, Yano M, Gratton JP. Block of endothelin-1-induced release of thromboxane A_2 from the guinea pig lung and nitric oxide from the rabbit kidney by a selective ET_B receptor antagonist, BQ-788. *Br J Pharmacol*. 1994;113:1257-1262.
11. de Nucci G, Thomas R, D'Orléans-Juste P, et al. Pressor effects of circulating endothelin are limited by its removal in the pulmonary circulation and by the release of prostacyclin and endothelium-derived relaxing factor. *Proc Natl Acad Sci U S A*. 1988;85:9797-9800.
12. Maurice MC, Gratton JP, D'Orléans-Juste P. Pharmacology of two novel mixed ET_A/ET_B receptor antagonists, BQ-928 and 238, in the carotid and pulmonary arteries and the perfused kidney of the rabbit. *Br J Pharmacol*. 1997;120:319-325.
13. Kilkenny C, Browne W, Cuthill IC, Emerson M, Altman DG, Group NCRRGW. Animal research: reporting in vivo experiments: the ARRIVE guidelines. *Br J Pharmacol* 2010;160:1577-1579.
14. McGrath JC, Lilley E. Implementing guidelines on reporting research using animals (ARRIVE etc.): new requirements for publication in BJP. *Br J Pharmacol*. 2015;172:3189-3193.
15. Angus JA, Wright CE. Techniques to study the pharmacodynamics of isolated large and small blood vessels. *J Pharmacol Toxicol Meth*. 2000;44:395-407.
16. Mulvany MJ, Halpern W. Contractile properties of small arterial resistance vessels in spontaneously hypertensive and normotensive rats. *Circ Res*. 1977;41:19-26.
17. Clozel M, Breu V, Gray GA, et al. Pharmacological characterization of bosentan, a new potent orally active nonpeptide endothelin receptor antagonist. *J Pharmacol Exp Ther*. 1994;270:228-235.
18. Curtis MJ, Bond RA, Spina D, et al. Experimental design and analysis and their reporting: new guidance for publication in BJP. *Br J Pharmacol*. 2015;172:3461-3471.
19. Bremnes T, Paasche JD, Mehlum A, Sandberg C, Bremnes B, Attramadal H. Regulation and intracellular trafficking pathways of the endothelin receptors. *J Biol Chem*. 2000;275:17596-17604.
20. Paasche JD, Attramadal T, Sandberg C, Johansen HK, Attramadal H. Mechanisms of endothelin receptor subtype-specific targeting to distinct intracellular trafficking pathways. *J Biol Chem*. 2001;276:34041-34050.
21. Stone M, Angus JA. Developments of computer-based estimation of pA_2 values and associated analysis. *J Pharmacol Exp Ther*. 1978;207:705-718.
22. Lew MJ, Angus JA. Analysis of competitive agonist-antagonist interactions by nonlinear regression. *Trends Pharmacol Sci*. 1995;16:328-337.
23. Clark AJ. The antagonism of acetyl choline by atropine. *J Physiol (Lond)*. 1926;61:547-556.
24. Wessale JL, Adler AL, Novosad EI, et al. Pharmacology of endothelin receptor antagonists ABT-627, ABT-546, A-182086 and A-192621: ex vivo and in vivo studies. *Clin Sci (Lond)*. 2002;103(Suppl 48):112S-117S.
25. Davenport AP, Hyndman KA, Dhaun N, et al. Endothelin. *Pharmacol Rev*. 2016;68:357-418.
26. Clozel M, Breu V, Burri K, et al. Pathophysiological role of endothelin revealed by the first orally active endothelin receptor antagonist. *Nature*. 1993;365:759-761.
27. Angus JA, Soeding PF, Hughes RJA, Wright CE. Functional estimation of endothelin-1 receptor antagonism by bosentan, macitentan and ambrisentan in human pulmonary and radial arteries in vitro. *Eur J Pharmacol*. 2017;804:111-116.
28. McCulloch KM, Docherty CC, Morecroft I, MacLean MR. Endothelin$_B$ receptor-mediated contraction in human pulmonary resistance arteries. *Br J Pharmacol*. 1996;119:1125-1130.
29. Hay DW, Luttmann MA, Beck G, Ohlstein EH. Comparison of endothelin B (ET_B) receptors in rabbit isolated pulmonary artery and bronchus. *Br J Pharmacol*. 1996;118:1209-1217.
30. Sauvageau S, Thorin E, Villeneuve L, Dupuis J. Change in pharmacological effect of endothelin receptor antagonists in rats with

pulmonary hypertension: role of ET_B-receptor expression levels. *Pulm Pharmacol Ther*. 2009;22:311-317.

31. Bauer M, Wilkens H, Langer F, Schneider SO, Lausberg H, Schäfers HJ. Selective upregulation of endothelin B receptor gene expression in severe pulmonary hypertension. *Circulation*. 2002;105:1034-1036.
32. Kelland NF, Kuc RE, McLean DL, et al. Endothelial cell-specific ET_B receptor knockout: autoradiographic and histological characterisation and crucial role in the clearance of endothelin-1. *Can J Physiol Pharmacol*. 2010;88:644-651.
33. Bolli MH, Marfurt J, Grisostomi C, et al. Novel benzo[1,4]diazepin-2-one derivatives as endothelin receptor antagonists. *J Med Chem*. 2004;47:2776-2795.
34. Iglarz M, Binkert C, Morrison K, et al. Pharmacology of macitentan, an orally active tissue-targeting dual endothelin receptor antagonist. *J Pharmacol Exp Ther*. 2008;327:736-745.
35. Breu V, Clozel M, Burri K, Hirth G, Neidhart W, Ramuz H. In vitro characterisation of Ro 46-8443, the first non-peptide antagonist selective for the endothelin ET_B receptor. *FEBS Lett*. 1996;383:37-41.
36. Cramer H, Müller-Esterl W, Schroeder C. Subtype-specific desensitization of human endothelin ET_A and ET_B receptors reflects differential receptor phosphorylation. *Biochemistry*. 1997;36:13325-13332.

How to cite this article: Angus JA, Hughes RJA, Wright CE. Distortion of K_B estimates of endothelin-1 ET_A and ET_B receptor antagonists in pulmonary arteries: Possible role of an endothelin-1 clearance mechanism. *Pharmacol Res Perspect*. 2017;e00374. https://doi.org/10.1002/prp2.374